

# Coherent Emission from the Nonpolar Optical Phonon of Diamond

Cornelius Beckh, Niklas Fritzsche, and Alfred Leitenstorfer

Department of Physics and Center for Applied Photonics, University of Konstanz, 78457 Konstanz, Germany

**Emission of a coherent field transient from optical phonons in monocrystalline diamond is observed after impulsive femtosecond excitation. Measurements on an extremely pure sample suggest a monoatomic layer of surface dipoles as a leading source for this subtle effect.**

## I. INTRODUCTION

OWING to the strong binding forces between relatively light atoms, the crystal lattice of diamond resides largely in its ground state even at room temperature [1]. Consequently, time-resolved studies of phonon excitations in this “quantum” material are numerous with a long tradition spanning close to five decades [2-4]. The strictly nonpolar character of the diatomic unit cell renders transverse- and longitudinal-optical modes degenerate in the center of the Brillouin zone and nominally infrared inactive. Consequently, coherent optical phonons in diamond have so far been excited and probed only via Raman scattering or other nonlinear-optical processes of odd order. In contrast to impulsively excited materials with partially ionic binding where coherent infrared emission from optical phonon polaritons is readily observable [5], it should be completely absent in nonpolar diamond. Nevertheless, when searching for distortions of the quantum vacuum due to few-femtosecond pumping, we observed a weak but unambiguous coherent field amplitude at the optical phonon frequency emitted by this fully covalent and centrosymmetric system.

## II. EXPERIMENTAL SETUP AND RESULTS

First, a  $\langle 110 \rangle$ -oriented sample of natural diamond with a thickness of  $d = 35 \mu\text{m}$  and a concentration of N impurities between 20 and 30 ppm is studied under normal incidence. We excite with 10-fs near-infrared pulses of an energy up to 40 nJ which are derived from a fiber-based parametric amplifier operating at a repetition rate of 10 MHz. After the sample, a Ge wafer inserted under Brewster’s angle spatiotemporally superimposes any emitted THz radiation with a 7.7-fs probe at a repetition rate of 20 MHz. Subsequently, both pulse trains are focused into an 18.8- $\mu\text{m}$ -thick gallium selenide (GaSe) electro-optic detector. Here, a co-propagating THz field amplitude induces a change in ellipticity of the probe pulses which we analyze at the Nyquist limit with a radio-frequency lock-in amplifier.

The black graph in Fig. 1(a) shows the electro-optic signal (EOS) of a coherent field transient emitted by the sample over an interval of time delays up to 10 ps. A damped sine function (blue) with a carrier frequency of 39.47 THz and an exponential decay time of 4.67 ps fits excellently to the transient. Due to the exquisite sensitivity of our setup, we can clearly resolve these oscillations with a peak field of approximately 1 V/cm. This value is four orders of magnitude lower as compared to the emission from an efficient optical rectification source with strong second-order nonlinearity and similar thickness. The power spectrum of the transient is depicted in Fig. 1(b). It

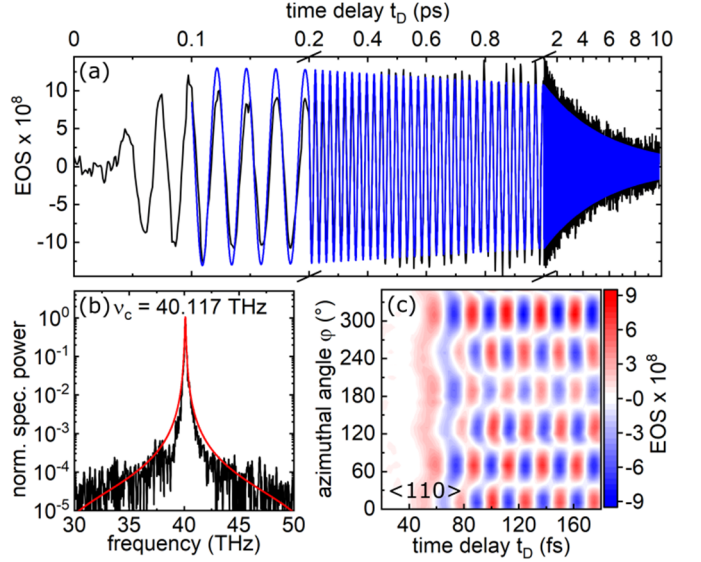


**Fig. 1.** (a) Electric field amplitude emitted after femtosecond excitation of a monocrystalline diamond sample oriented along the  $\langle 110 \rangle$  direction, as detected by electro-optic sampling in a GaSe sensor. (b) Power spectrum (black) of the transient in (a), as obtained by fast Fourier transform. Red line: Lorentzian fit. (c) Emitted field amplitude color-coded versus in-plane angle of sample orientation and delay time.

exhibits a narrow peak with a center frequency of  $\nu_c = 40.12$  THz towering more than 40 dB above the noise floor. Note that both the center frequency deduced from the Fourier spectrum and the carrier of the sinusoidal fit are very close to the literature value for the Raman frequency of the zone-center optical phonon in diamond of 39.95 THz [6].

The EOS at early time delays is depicted in Fig. 1(c) when rotating the emitter crystal around the optical propagation axis with the azimuthal angle  $\phi$ . The regular modulations of the oscillatory part of the emission are compatible with the symmetry of the undistorted lattice seen in the  $\langle 110 \rangle$  direction. Note that the emission is present in all monocrystalline diamond samples we have studied so far, some of them oriented in different directions and with lower impurity concentrations. To access the fundamental physics of these phenomena, we look at an emitter crystal at the highest symmetry and level of purity available to us.

An electronic-grade diamond sample grown by chemical vapor deposition (CVD) and oriented in the  $\langle 100 \rangle$  direction has a similar thickness of  $d = 29 \mu\text{m}$  as the natural  $\langle 110 \rangle$  sample. The impurity concentration of less than 2 ppb is more than four orders of magnitude below the one of the first specimen. The emitted field amplitude under normal incidence exhibits a somewhat smaller amplitude and, most likely, the higher purity leads to a smaller damping of the coherent phonon oscillation. From an EOS measurement over a time interval of 15 ps, an exponential decay time of 7.14 ps is determined and the Fourier spectrum is centered at a frequency of  $\nu_c = 40.005$  THz. In Fig. 2(a), the early time delays of the EOS are depicted when rotating the specimen around the optical propagation axis, as it

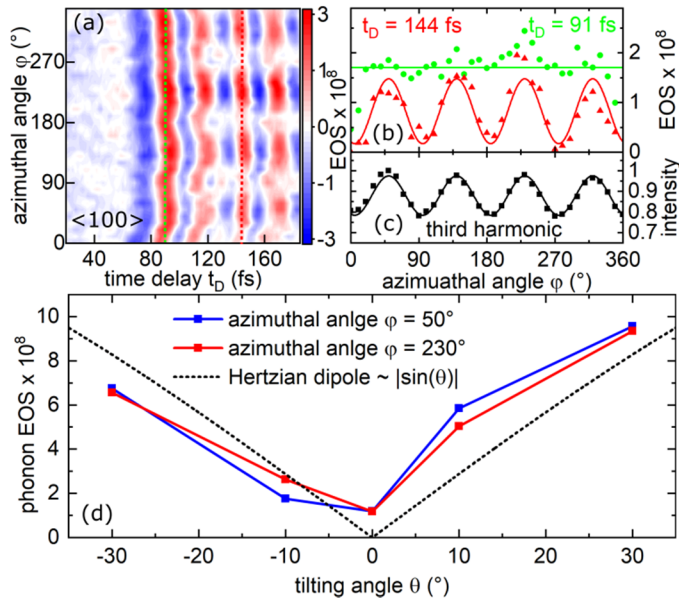


**Fig. 2** Measurements of  $\langle 100 \rangle$ -oriented diamond with impurity level below 2 ppb. (a) Emitted field amplitude color-coded versus in-plane angle of sample orientation and delay time  $t_D$ . (b) Two cuts through the color map in (a) for two fixed delay times. The amplitude at  $t_D = 91$  fs is plotted as green dots versus the in-plane angle. At  $t_D = 144$  fs, the signal amplitude is plotted with red triangles together with a sine function of a period of  $90^\circ$ . (c) Normalized third-harmonic intensity emitted from the high-purity diamond sample versus in-plane angle together with a fit to a sine function (black squares and solid line). (d) The maximum phonon amplitude for two different in-plane angles (red and blue) are plotted for five tilting angles between  $\theta = -30^\circ$  and  $30^\circ$ . The black dashed line indicates the qualitative behavior expected for emission by a Hertzian dipole oriented perpendicular to the sample surface.

is shown in Fig. 1(c) for the natural  $\langle 110 \rangle$ -cut sample. Between time delays of 60 fs and 110 fs, the emitted amplitude is almost constant for a full rotation around the propagation direction. This behavior is depicted in green in Fig. 2(b), showing the signal amplitudes of a cut through the color map at a delay time of  $t_D = 91$  fs. The frequency content of this angle-independent oscillation with a duration of approximately 50 fs reaches from 10 THz to 50 THz. Therefore, some sort of nonlinear-optical rectification process of second order related to the symmetry break at the sample surface might be the origin. A linear increase of the emitted electric field amplitude with excitation power fits to this assumption.

In the measurement depicted in Fig. 2(a), the amplitude of the phonon oscillation is smaller than the initial angle-independent amplitude and starts approximately at time delays beyond 120 fs. A fourfold symmetry of the phonon amplitude versus the in-plane angle of the emitter crystal is obvious. A cut through the color map at a delay time of  $t_D = 144$  fs illustrates the angle dependence of the oscillation (red triangles) and a sine-function fit with a period of  $90^\circ$  matches the data points well (red line). An analogous behavior for  $\langle 100 \rangle$ -oriented diamond is known from the generation process of coherent phonons by impulsive stimulated Raman scattering (ISRS), consistent with the off-diagonal Raman tensor of the optical phonons with  $\Gamma_{25'}$  symmetry [3]. For checkup, we determine the crystal orientation detecting the intensity of the third harmonic of the excitation pulse. As expected, and seen in Fig. 2(c), it exhibits the same fourfold symmetry. The modulation period and depth of the third-harmonic intensity is derived from the susceptibility tensor of third order and the corresponding nonlinear

parameters [7]. Furthermore, the amplitude of the emitted phonon oscillation field depends linearly on the excitation power for all samples, also consistent with the ISRS generation process of coherent phonons. We record that the rotational symmetry under normal incidence and the power dependence of the emitted field is directly connected to the generation of the coherent phonon in the bulk.

To investigate the origin of the coherent emission from the phonon oscillation in nonpolar diamond further, the electronic grade  $\langle 100 \rangle$  sample is tilted away from normal incidence by angles of  $\theta = -30^\circ, -10^\circ, 0^\circ, 10^\circ$  and  $30^\circ$ . The maximum EOS amplitudes of the phonon oscillation are plotted versus the polar angle  $\theta$  in Fig. 2(d). For positive and negative angles, the amplitude increases, in agreement with the assumption of a significant contribution by some kind of oscillating dipole perpendicular to the surface. The dashed line qualitatively illustrates the angle-dependent amplitude of the electric field emitted by a Hertzian dipole oscillating parallel to the surface normal. For other samples with higher impurities, we found a more complex behavior. Therefore, we first considered an intrinsic bulk effect like e.g. influences of higher-order emission multipoles beyond the dipole approximation.

So far, it seems clear that a generation of the longitudinal coherent phonon oscillation at a frequency of 40 THz takes place by impulsive stimulated Raman scattering. Hence, the carbon atoms at the surface of the diamond oscillate in the direction of propagation. In contrast to the bulk, the surface atoms have dangling bonds which may be saturated by H or other atomic species. Differences in electronegativity between these surface-terminating atoms and the bulk lattice create a dipole moment perpendicular to the surface in the order of 0.1 eÅ [8]. The results in Fig. 2(d) indicate that this tiny monoatomic dipole sheet might be the origin of the emitted field. Our experimental data on less pure samples show that any influences leading to a break of inversion symmetry like concentration gradients of bulk impurities, internal stress or grain boundaries could cause a more complicated angular dependence of the amplitude of the coherent emission. Definitely, it is interesting to see that, within our spectral resolution, the surface dipole oscillates exactly at the frequency of the bulk optical phonon mode in the zone center. In any case, our findings provide a new route to study structural dynamics in diamond and they are important for applications of this important material in time-domain quantum optics.

## REFERENCES

- [1] H.M.J. Smith and M. Born, "The theory of the vibrations and the Raman spectrum of the diamond lattice," *Trans. Roy. Soc. A* **241**, 105 (1947).
- [2] A. Laubereau, D. von der Linde, and W. Kaiser, "Decay Time of Hot TO Phonons in Diamond," *Phys. Rev. Lett.* **27**, 802 (1971).
- [3] K. Ishioka, M. Hase, and M. Kitajima, "Coherent optical phonons in diamond," *Appl. Phys. Lett.* **89**, 231916 (2006).
- [4] S. Mährlein et al., "Terahertz Sum-Frequency Excitation of a Raman-Active Phonon," *Phys. Rev. Lett.* **119**, 127402 (2017).
- [5] A. Leitenstorfer et al., "Femtosecond Charge Transport in Polar Semiconductors," *Phys. Rev. Lett.* **82**, 5140 (1999).
- [6] C.A. Klein, T.M. Hartnett, and C.J. Robinson, "Critical-point phonon frequencies of diamond," *Phys. Rev. B* **45**, 12854 (1992).
- [7] X. Yang, S. Xie, "Expression of third-order effective nonlinear susceptibility for third-harmonic generation in crystals," *Appl. Opt.* **34**, 6130-6135 (1995).
- [8] J. Ristein, "Diamond surfaces: familiar and amazing," *Appl. Phys. A* **82**, 377-384 (2006).